Dynamic mean-field theory and the like

Jinyuan Wu

March 26, 2023

Abstract

Mapping a highly localized many-body strongly correlated electronic system to an impurity problem is possible, which motivates the development of DMFT as a numerical approach to such systems. This report reviews the theory foundation of DMFT, its improved versions, and DFT+DMFT and GW+DMFT *ab initio* methods.

1 Introduction

Suppose we are to find the single-particle Green function of a condensed matter system. The standard procedure is to find the irreducible self-energy Σ by Feynman diagram resummation. In strongly correlated systems, deciding diagrams with most contributions is generally hard, and brutal-force resummation proves intractable. Besides, there are subtleties concerning the well-definedness and uniqueness of Feynman diagram resummation techniques. When dealing with truly strongly correlated systems, attention should be paid to avoiding going into an unphysical branch [1, 2].

If, however, it is found that the self-energy (or two-particle vertex, or similar "n-particle self-energy diagrams") is highly local, then in principle, the self-energy can be replicated in a *few-body* model, or as we are going to see below, a *many-body impurity model* in Hamiltonian formalism. Suppose, for example, that the real space self-energy $\Sigma_{\boldsymbol{ij}}$ is only important when $|\boldsymbol{i}-\boldsymbol{j}| \leq n$. Then we can just choose a cluster of sites satisfying the $|\boldsymbol{i}-\boldsymbol{j}| \leq n$ condition, and integrate out the rest of electron modes, and in the resulting impurity model, $\Sigma_{\boldsymbol{ij}}$ is exactly the same as in the original model. The main obstacle now is to decide the parameters in this new impurity model, which can be solved by adopting a self-consistent scheme: $\Sigma_{\boldsymbol{ij}}$, together with the free part of the original model, decides the one-particle Green function, which then can be used to fit the parameters in the impurity model, and then the impurity model can be solved to update the self-energy.

It can be seen that diagrammatically speaking, this idea is also a resummation strategy, though here we truncate diagrams according to their *locality* instead of structures, and the local parts of *all* diagrams, as long as they fit in the ansatz of the impurity model, are included when we solve the impurity model. This can also be seen as a mean-field approach, just like other self-consistent Feynman diagram resummation strategies. Since the parameters in the impurity model may contain time explicitly, we may say what we are doing is a *dynamic* mean-field theory.

This report reviews the development of dynamic mean-field theory (DMFT). The term *dynamic mean-field theory* is usually reserved for the most coarse approximation with a single-site cluster and a completely space-independent self-energy discussed in Section 2. In Section 3, we move beyond the simplest DMFT scheme and increase the number of sites and loose the locality requirement for the self-energy. Section 4 is about combining DMFT and *ab initio* methods together.

2 DMFT for the Hubbard model

2.1 Duality between the Hubbard model and the Anderson impurity model

In this section we discuss DMFT for the Hubbard model

$$H = -t \sum_{\langle \boldsymbol{i},\boldsymbol{j}\rangle,\sigma} c^\dagger_{\boldsymbol{i}\sigma} c_{\boldsymbol{j}\sigma} + \text{h.c.} + U \sum_{\boldsymbol{i}} n_{\boldsymbol{i}\uparrow} n_{\boldsymbol{j}\downarrow} - \mu N. \tag{1}$$

The free part results in the imaginary time Green function

$$G_0(\mathrm{i}\omega_n, \boldsymbol{k}\sigma) = G_0(\mathrm{i}\omega_n, \boldsymbol{k}), \quad G_0(\mathrm{i}\omega_n, \boldsymbol{k}) = \frac{1}{\mathrm{i}\omega_n - \varepsilon_{\boldsymbol{k}} + \mu}, \tag{2}$$

where $\varepsilon_{\boldsymbol{k}}$ is the band structure of the tight-binding model part. Now we map the Hubbard model to an impurity theory. We keep only one site in the impurity theory and integrate out the rest, and the final effective theory looks like

$$S_{\text{single site}} = -\int \mathrm{d}\tau \int \mathrm{d}\tau'\, \bar{c}(\tau)\mathcal{G}^{-1}(\tau - \tau')c(\tau') + \int \mathrm{d}\tau\, U n_\uparrow(\tau) n_\downarrow(\tau). \tag{3}$$

The Green function $\mathcal{G}(\tau)$ is $G_{0,\boldsymbol{ii}}(\tau)$ corrected by the integrated out electronic degrees of freedom; the local interaction $Un_\uparrow n_\downarrow$ is not included in $\mathcal{G}$.

Note that $\mathcal{G}$ can also be seen as a single-particle Green function with self-energy correction, and therefore has the same structure of a self-energy-corrected single-particle Green function, although its value is different from $G_{\boldsymbol{ii}}$, because its self-energy is different from the self-energy of the whole Hubbard system, since the former only considers sites beside $\boldsymbol{i}$ while the latter considers all sites. Assuming the self-energy of $\mathcal{G}$ is well-behaved for Hilbert transformation [3], we write the structure of $\mathcal{G}$ as

$$\mathcal{G}(\mathrm{i}\omega_n)^{-1} = \mathrm{i}\omega_n + \text{const.} + \int \mathrm{d}\epsilon\, g(\epsilon) \frac{1}{\mathrm{i}\omega_n - \epsilon},$$

and this means the single-site model can be instantiated by replacing $\mathcal{G}$ by a bath of non-interactive electrons, the dispersion relations of which are decided by poles of $\mathcal{G}$, and we get an Anderson impurity model

$$H_{\text{Anderson}} = \underbrace{\epsilon_0 \sum_\sigma c_\sigma^\dagger c_\sigma + \sum_{\boldsymbol{k},\sigma} E_{\boldsymbol{k}} d_{\boldsymbol{k}\sigma}^\dagger d_{\boldsymbol{k}\sigma} + \sum_{\boldsymbol{k}} (V_{\boldsymbol{k}} d_{\boldsymbol{k}\sigma}^\dagger c_\sigma + \text{h.c.})}_{\simeq c^\dagger \mathcal{G} c} + U n_\uparrow n_\downarrow. \tag{4}$$

The structure of $\mathcal{G}$ is therefore

$$\mathcal{G}(\mathrm{i}\omega_n) = \frac{1}{\mathrm{i}\omega_n - \epsilon_0 - \Delta(\mathrm{i}\omega_n)}, \quad \Delta(\mathrm{i}\omega_n) = \sum_{\boldsymbol{k}} \frac{|V_{\boldsymbol{k}}|^2}{\mathrm{i}\omega_n - E_{\boldsymbol{k}}}. \tag{5}$$

Note that the influence of $Un_\uparrow n_\downarrow$ is not accounted for by $\mathcal{G}$. Other Hamiltonian realizations of (3) are of course possible [3]. Note that here Δ contains explicitly $\mathrm{i}\omega_n$ and therefore has retardation effects in the real space. Therefore (3) contains retardation, and this is an evidence why it is better to put it into the form of a *many-body* impurity model instead of a single-body model.

We use G_{imp} to refer to the interaction-corrected Green function in the impurity model. Note that by definition of the mapping, we have $G_{\text{imp}}(\mathrm{i}\omega_n) = G_{\boldsymbol{ii}}(\mathrm{i}\omega_n)$, and therefore

$$\frac{1}{\mathcal{G}(\mathrm{i}\omega_n)^{-1} - \Sigma_{\text{imp}}} = G_{\text{imp}}(\mathrm{i}\omega_n) = G_{\boldsymbol{ii}}(\mathrm{i}\omega_n) = \frac{1}{N}\sum_{\boldsymbol{k}} G(\mathrm{i}\omega_n, \boldsymbol{k}) = \frac{1}{N}\sum_{\boldsymbol{k}} \frac{1}{\mathrm{i}\omega_n - \epsilon_{\boldsymbol{k}} - \Sigma(\mathrm{i}\omega_n, \boldsymbol{k})}. \tag{6}$$

where G is the fully corrected Green function in the Hubbard model, Σ is the self-energy of the Hubbard model, and Σ_{imp} is the self-energy correction to $\mathcal{G}$ caused by $Un_\uparrow n_\downarrow$.

2.2 The self-energy locality condition

The mapping from a Hubbard model to an Anderson impurity model involves no physical approximation. Now we impose the locality condition of the self-energy mentioned in the introduction: we assume the Hubbard model self-energy $\Sigma(\mathrm{i}\omega_n, \boldsymbol{k})$ is highly localized in the real space, and therefore involves no $\boldsymbol{k}$-dependence, and thus we immediately get

$$\Sigma_{\text{imp}} = \Sigma(\mathrm{i}\omega_n \boldsymbol{k}). \tag{7}$$

This approximation is exact in an infinite lattice [4], and therefore expectedly works better for bulk materials than monolayer materials.

2.3 The self-consistent loop

The cutoff (7) gives us a self-consistent calculation scheme: first using G_0 (known) and Σ_{imp} (from last iteration), we have

$$G(\mathrm{i}\omega_n, \boldsymbol{k}) = \frac{1}{\mathrm{i}\omega_n - \varepsilon_{\boldsymbol{k}} + \mu - \Sigma_{\text{imp}}(\mathrm{i}\omega_n)}, \tag{8}$$

and then we calculate $G_{\boldsymbol{ii}}$ (essentially G_{imp}) by

$$G_{\boldsymbol{ii}}(\mathrm{i}\omega_n) = \frac{1}{N}\sum_{\boldsymbol{k}} G(\mathrm{i}\omega_n, \boldsymbol{k}), \tag{9}$$

and then $\mathcal{G}$ can be found by

$$\mathcal{G}(\mathrm{i}\omega_n)^{-1} = G_{\boldsymbol{ii}}(\mathrm{i}\omega_n)^{-1} + \Sigma_{\text{imp}}(\mathrm{i}\omega_n). \tag{10}$$

Now the impurity model is fully determined, and with U and $\mathcal{G}(\mathrm{i}\omega_n)$, we solve the impurity model by calling an existing impurity solver and get G_{imp}. So now G_{imp} is updated, and we can then find the updated Σ_{imp}, and we go back to the starting point of the loop.

Note that here Σ_{imp} is *not* calculated using diagrammatic resummation techniques. Instead, we find G_{imp} without explicitly mentioning Σ_{imp} in the impurity solver step, and Σ_{imp} is found *after* G_{imp} (and $\mathcal{G}$) is known. This guarantees enough accuracy of Σ_{imp}: if it is evaluated in the same way with, say, the GW method, infinite diagrams are thrown away, but here *all* Feynman diagrams contributing to Σ_{imp} – and therefore $\Sigma(\mathrm{i}\omega_n, \boldsymbol{k})$ – are taken into account; what is ignored is just their spatial independent parts.

For Hubbard model, the interaction term in the impurity problem is exactly $Un_\uparrow n_\downarrow$, because it is strictly local and is not corrected when electrons on other sites are integrated out. For models with nearest-neighbor interaction, this is no longer correct, because now integrating out other electron modes means screening of the interaction. An even more important fact about models with repulsion between electrons from different sites is the interaction term cannot appear in a single-site model. To solve the above problems, a possible way is to use a Hubbard-Stratonovich transformation and use an auxiliary boson field to introduce the interaction. The resulting single-site model is in an itinerant electron bath and a bosonic bath [5].

3 Going beyond DMFT

Unfortunately, in some scenarios the original single-site DMFT is bound to fail. This is exemplified in phrase transition, in which long-wavelength behaviors are highly important, and a strictly local Σ cannot be the case. A possible direction of improvement is to use an impurity dual Hamiltonian involving a larger cluster of states [6, 7]. The main problem of this approach is the speed: the impurity model concerning a large impurity cluster has to be solved with high accuracy, and this is demanding for existing solvers [8, 9].

Improvement can also be made by relaxing the strict locality condition for the self-energy, which leads to the dynamic vertex approximation. In the dynamic vertex approximation (DΓA), we assume that Σ is not local, but the two-particle vertex Γ is local. The spatial-varying self-energy can then be calculated from Γ [10]. Consider Fig. 1(a): a diagram in the self-energy always starts with a Coulomb interaction vertex, so all self-energy diagrams can be seen as a Coulomb vertex plus a four-legged diagram. When the four-legged diagram is disconnected, we only have two diagrams that are logically possible, and we can find they are just the Hartree diagram and the Fock diagram, and the propagators inside are modified by self-energy correction (Fig. 1(b)). When there is at least one Coulomb interaction line connecting the upper lines and the lower lines of the four-leg diagram, the four legs have to be linked to four self-energy-corrected electron lines, or otherwise the diagram is not well-formed. Thus we find the sum of all diagrams besides diagrams in (b) is proportion to the reducible two-particle vertex diagram (c), and (a) = (b) + (c) [10]. Specifically, the reducible two-particle vertex diagram contains two diagrams (d) and (e), and they correspond to a term in the screening correction (i.e. correction of the interaction line, or "vacuum polarization" in terms of particle physics) and a term in the vertex correction, both of which are expected self-energy diagrams. Thus, in DΓA, we can self-consistently update the Γ function, i.e. the two-particle vertex function, which already contains all the information of the single-electron self-energy.

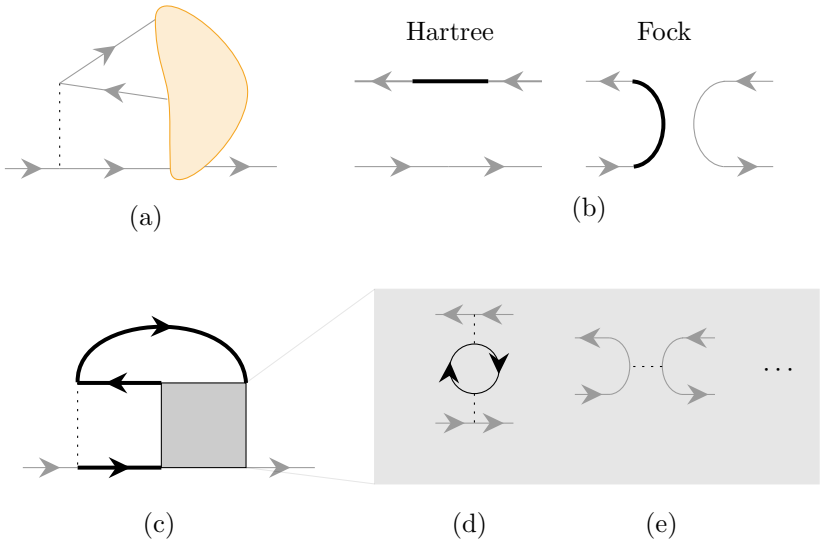

Figure 1: Finding the self-energy from the reducible vertex function. Here grey lines are external lines, which do not contribute propagator factors and merely provides a momentum value when the diagram is evaluated; bold lines are lines with interaction correction, like self-energy correction for electron lines. (a) The schematic illustration of the structure of all self-energy diagrams. (b) Two simplest self-energy diagrams. (c) The structure of all self-energy diagrams besides the two in (b). The grey box is the two-particle irreducible vertex. (d, e) Two examples of the content of the two-particle irreducible vertex.

4 DMFT in *ab initio* calculation

As is mentioned above, DMFT (and even its improved versions) assumes strong locality conditions to the system, and therefore has inherent difficulties to capture itinerant behaviors. Common *ab initio* band structure calculation approaches, including DFT and GW, on the other hand, do not capture localized behaviors. Mixing DFT or GW with DMFT is therefore needed for large-scale *ab initio* simulation of materials involving electron localization, or in other words, magnetism.

All electronic structure calculation approaches that use the quasiparticle picture can be summarized as an instance of the minimization problem of the functional

$$\Omega[\mathbf{G}] = \Phi[\mathbf{G}] + \operatorname{Tr}\ln(-\mathbf{G}) - \operatorname{Tr}\left(\left(\mathbf{G}_0^{-1} - \mathbf{G}^{-1}\right)\mathbf{G}\right) \tag{11}$$

with respect to the matrix form of the renormalized Green function G, where Ω is the grand potential and equals $E - \mu N$ at $T = 0$, and the Luttinger-Ward functional Φ is the sum of of all closed, irreducible, and renormalized skeleton diagrams, and we have

$$\mathbf{\Sigma} = \frac{\delta\Omega}{\delta\mathbf{G}}, \tag{12}$$

so Φ and Ω are some kinds of generating functionals [11, 12].

Specifically, Kohn-Sham density functional theory (DFT) can be formulated in the framework of Luttinger-Ward functional: the Kohn-Sham orbitals are "wave functions" appearing in the spectral representation of the one-particle Green function, and the exchange-correlation functional is Φ in terms of the electron number density. In principle, this means the exchange-correlation functional used in DFT can be improved systematically using Feynman diagrammatic techniques [13, 14, 15], although the infamous semiconductor band gap problem persists even with an accurate functional (and actually becomes worse because now there is no cancellation of errors), because we still need to consider the contribution of energy functional discontinuity [14]. The idea that the density functional can be obtained from Feynman diagrams however is important when we need to develop brand-new DFTs for systems like, say, superconductors and exciton insulators, in which interaction channels other than Coulomb interaction exist and

no past experience is there for reference; in that case, summing up several low-order bubble diagrams and using the result as an initial guess for the energy functional may be one way to proceed [16, 17].

On the other hand, the DMFT version of Φ is

$$\Phi = \sum_{\boldsymbol{i}} \Phi^{U}_{\text{single site}}[G_{\text{imp},\boldsymbol{i}}], \tag{13}$$

in which we sum over all atoms in the crystal to make Φ an extensive quantity, and indeed, we can show that when $d \to \infty$, (13) is exact, in order to justify DMFT in the $d \to \infty$ limit [3]. Therefore to mix DMFT with DFT, we need to replace the part in Φ_{DFT} that could be better described by DMFT, and the resulting Luttinger-Ward functional is

$$\Phi[G] = \Phi_{\text{DFT}}[G] + \Phi_{\text{DMFT}}[G_{\text{loc}}] - \Phi_{\text{DC}}[G], \tag{14}$$

where the subscript loc means to replace $G_{\boldsymbol{ij}}$ by $G_{\boldsymbol{ii}}$, and Φ_{DC} means double-counting and can be evaluated exactly [18], and the Hubbard U can be calculated by considering the Coulomb interaction screened by electrons not governed by DMFT. Similarly, we can also design a GW+DMFT scheme, where

$$\Phi[G] = \Phi_{GW}[G] + \Phi_{\text{DMFT}}[G_{\text{loc}}] - \Phi_{\text{Hubbard } GW}[G_{\text{loc}}]. \tag{15}$$

Here the double counting term (the third term) can be evaluated more explicitly, because DMFT considers the local, Hubbard-like versions of all GW diagrams, so to avoid double counting, we can just skip these diagrams. The self-consistent equations can be found by taking the variation of these functionals.

5 Conclusion and discussion

Diagrammatic approaches in computational condensed matter physics usually truncate diagrams according to the number of interaction vertices (MP2, MP3) or according to the structure of the diagrams (RPA, GW) [19, 20]. DMFT, on the other hand, utilizes the *locality* condition, and hence maps an intractable many-body problem into a hard yet tractable impurity problem. This makes it especially important for strongly-correlated magnetic systems, where itinerant behaviors are absent.

Despite being a method originally designed for effective models, among other numerical approaches to strongly correlated electronic systems, DMFT is remarkable for operating well with *ab initio* methods (DMRG also appears in *ab initio* calculations, but only for molecules [21]). DFT+U is another attempt to mix ideas from effective models to *ab initio* calculation, but it only works well when the electrons remain itinerant [22]. DFT+DMFT, on the other hand, is able to capture electron localization.

The bottleneck of DMFT seems to be the impurity solver, with new solvers still being reported and discussed [23, 24, 25, 26]. The existing approaches include exact diagonalization, quantum Monte Carlo, another diagrammatic resummation scheme (this time for the impurity problem), and more. The development of DMFT is by no means finished, and further work is needed for achieving the balance between accuracy and speed.

References

[1] O. Gunnarsson et al. “Breakdown of Traditional Many-Body Theories for Correlated Electrons”. In: *Phys. Rev. Lett.* 119 (5 2017), p. 056402.

[2] Evgeny Kozik, Michel Ferrero, and Antoine Georges. “Nonexistence of the Luttinger-Ward Functional and Misleading Convergence of Skeleton Diagrammatic Series for Hubbard-Like Models”. In: *Phys. Rev. Lett.* 114 (15 2015), p. 156402.

[3] Antoine Georges et al. “Dynamical mean-field theory of strongly correlated fermion systems and the limit of infinite dimensions”. In: *Rev. Mod. Phys.* 68.1 (1996), p. 13.

[4] Antoine Georges and Gabriel Kotliar. “Hubbard model in infinite dimensions”. In: *Phys. Rev. B* 45 (12 1992), pp. 6479–6483.

[5] Ping Sun and Gabriel Kotliar. "Extended dynamical mean-field theory and *GW* method". In: *Phys. Rev. B* 66.8 (2002), p. 085120.

[6] Gabriel Kotliar et al. "Cellular dynamical mean field approach to strongly correlated systems". In: *Phys. Rev. Lett.* 87.18 (2001), p. 186401.

[7] Hyowon Park, Kristjan Haule, and Gabriel Kotliar. "Cluster dynamical mean field theory of the Mott transition". In: *Phys. Rev. Lett.* 101.18 (2008), p. 186403.

[8] Michael Potthoff. "Cluster Extensions of Dynamical Mean-Field Theory". In: *DMFT: From Infinite Dimensions to Real Materials*. 2018, p. 20. URL: https://www.cond-mat.de/events/correl18/manuscripts/potthoff.pdf.

[9] Emanuel Gull et al. "Continuous-time Monte Carlo methods for quantum impurity models". In: *Rev. Mod. Phys.* 83.2 (2011), pp. 349–404.

[10] NE Bickers and SR White. "Conserving approximations for strongly fluctuating electron systems. II. Numerical results and parquet extension". In: *Phys. Rev. B* 43.10 (1991), p. 8044.

[11] J. M. Luttinger and J. C. Ward. "Ground-State Energy of a Many-Fermion System. II". In: *Phys. Rev.* 118 (5 1960), pp. 1417–1427.

[12] Michael Potthoff. "Self-energy-functional approach to systems of correlated electrons". In: *The European Physical Journal B-Condensed Matter and Complex Systems* 32.4 (2003), pp. 429–436.

[13] Ferdi Aryasetiawan, T Miyake, and K Terakura. "Total energy method from many-body formulation". In: *Phys. Rev. Lett.* 88.16 (2002), p. 166401.

[14] Myrta Grüning, Andrea Marini, and Angel Rubio. "Density functionals from many-body perturbation theory: The band gap for semiconductors and insulators". In: *The Journal of chemical physics* 124.15 (2006), p. 154108.

[15] Kristjan Haule and Turan Birol. "Free energy from stationary implementation of the DFT+ DMFT functional". In: *Phys. Rev. Lett.* 115.25 (2015), p. 256402.

[16] S Kurth et al. "Local density approximation for superconductors". In: *Physical review letters* 83.13 (1999), p. 2628.

[17] Hsiao-Yi Chen, Takuya Nomoto, and Ryotaro Arita. "Development of ab initio method for exciton condensation and its application to $TiSe_2$". In: *arXiv preprint arXiv:2208.10019* (2022).

[18] Kristjan Haule. "Exact double counting in combining the dynamical mean field theory and the density functional theory". In: *Phys. Rev. Lett.* 115.19 (2015), p. 196403.

[19] Xinguo Ren et al. "Random-phase approximation and its applications in computational chemistry and materials science". In: *Journal of Materials Science* 47.21 (2012), pp. 7447–7471.

[20] Fabien Bruneval, Nike Dattani, and Michiel J Van Setten. "The GW Miracle in Many-Body Perturbation Theory for the Ionization Potential of Molecules". In: *Frontiers in chemistry* 9 (2021).

[21] Alberto Baiardi and Markus Reiher. "The density matrix renormalization group in chemistry and molecular physics: Recent developments and new challenges". In: *The Journal of Chemical Physics* 152.4 (2020), p. 040903.

[22] Eva Pavarini. "Solving the strong-correlation problem in materials". In: *La Rivista del Nuovo Cimento* 44.11 (2021), pp. 597–640.

[23] C Weber et al. "Augmented hybrid exact-diagonalization solver for dynamical mean field theory". In: *Phys. Rev. B* 86.11 (2012), p. 115136.

[24] Martin Ganahl et al. "Efficient DMFT impurity solver using real-time dynamics with matrix product states". In: *Phys. Rev. B* 92.15 (2015), p. 155132.

[25] Ryota Mizuno, Masayuki Ochi, and Kazuhiko Kuroki. "Development of an efficient impurity solver in dynamical mean field theory for multiband systems: Iterative perturbation theory combined with parquet equations". In: *Phys. Rev. B* 104 (3 2021), p. 035160.

[26] Bruno Max de Souza Melo et al. “Quantitative comparison of Anderson impurity solvers applied to transport in quantum dots”. In: *Journal of Physics: Condensed Matter* 32.9 (2019), p. 095602.